ORIGINAL PAPER

Dynamics of microbubble oscillators with delay coupling

C.R. Heckman · R.H. Rand

Abstract Two vibrating bubbles submerged in a fluid influence each others' dynamics via sound waves in the fluid. Due to finite sound speed, there is a delay between one bubble's oscillation and the other's. This scenario is treated in the context of coupled nonlinear oscillators with a delay coupling term. It has previously been shown that with sufficient time delay, a supercritical Hopf bifurcation may occur for motions in which the two bubbles are in phase. In this work, we further examine the bifurcation structure of the coupled microbubble equations, including analyzing the sequence of Hopf bifurcations that occur as the time delay increases, as well as the stability of this motion for initial conditions which lie off the in-phase manifold. We show that in fact the synchronized, oscillating state resulting from a supercritical Hopf is attracting for such general initial conditions.

C.R. Heckman
Field of Theoretical and Applied Mechanics,
Cornell University, Ithaca, NY 14850, USA

R.H. Rand (✉)
Department of Mechanical and Aerospace Engineering and Department of Mathematics, Cornell University, Ithaca, NY 14850, USA
e-mail: rhr2@cornell.edu

1 Introduction

Delay is a widely exhibited phenomenon in dynamical systems, characterized by when a system's current state depends at least in part on its history. There are a wealth of examples of such systems, ranging from technological to biological. Coupled laser systems, high-speed milling, population dynamics, and gene expression are just a handful of examples where nonnegligible delay presents itself inherently in the dynamics of the system under study. This paper examines a system of coupled microbubbles, which are influencing each other via acoustic waves. Such studies are motivated in part by medical applications—in particular, the localized delivery of drugs via bubble transport. In this process, microbubbles filled with a drug are used as a vehicle for local delivery and are propagated to a target site by use of ultrasound forcing [1, 3, 9]. In such a scenario, it is desirable to have a complete picture of the dynamical behavior of interacting microbubbles in order to appropriately predict their motion, for instance, in a feedback system. Full understanding of the behavior of systems of coupled microbubbles involves taking into account the speed of sound in the liquid, which will lead to a delay in induced pressure waves between the bubbles in a cloud.
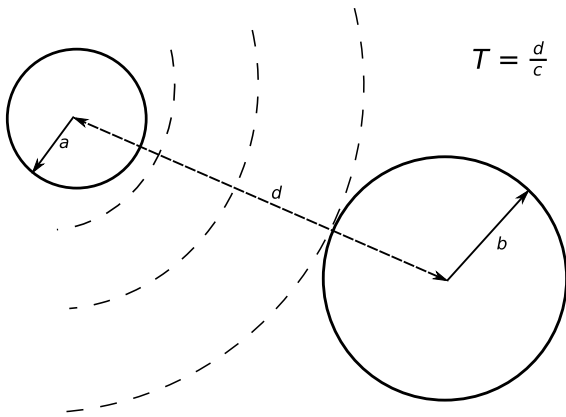
Fig. 1 Two bubbles submerged in a liquid. Note that bubble b also influences bubble a with an induced acoustic wave. Delay $T = d/c$ where d is the distance between bubbles and c is sound speed

We will provide here a very brief history of the study of microbubbles. The first modern analysis in bubble dynamics was made by Rayleigh [19]. His work on bubbles assumed an incompressible fluid with a constant background pressure, which has since been extended to models of bubble dynamics in a compressible fluid with time-dependent background pressure; see e.g., Plesset [13], Gilmore [4], Plesset and Prosperetti [14], and Joseph Keller and his associates [6, 7], as well as many contemporaries including, for instance, Lauterborn [8] and Szeri [20, 21] and others [2, 5, 11].

In this work, we consider the dynamics of a system of two delay-coupled bubble oscillators. The bubbles are modeled by the Rayleigh–Plesset equation, featuring a coupling term that is delayed as a result of the finite speed of sound in the fluid. A drawing of the physical phenomenon under study is presented in Fig. 1. Manasseh et al. [10] have studied coupled bubble oscillators without delay. The source of the delay comes from the time it takes for the signal to travel from one bubble to the other through the liquid medium, which surrounds them. Adding the coupling terms used in [10], the governing equations of the bubble system are:

$$(\dot{a} - c)\left(a\ddot{a} + \frac{3}{2}\dot{a}^2 - a^{-3\gamma} + 1\right) - \dot{a}^3$$
$$- (3\gamma - 2)a^{-3\gamma}\dot{a} - 2\dot{a} = P\dot{b}(t - T) \quad (1)$$

$$(\dot{b} - c)\left(b\ddot{b} + \frac{3}{2}\dot{b}^2 - b^{-3\gamma} + 1\right) - \dot{b}^3$$
$$- (3\gamma - 2)b^{-3\gamma}\dot{b} - 2\dot{b} = P\dot{a}(t - T) \quad (2)$$

where T is the delay and P is a coupling coefficient. Here we have omitted coupling terms of the form $P_1 b(t - T)$ and $P_1 a(t - T)$ from Eqs. (1), (2), where P_1 is a coupling coefficient [23]. Note that the equation follows the form explored by Keller et al. [6]. We have assumed that the coupling strength is constant, but a more realistic model could consider the coupling strength to be reduced with increasing distance, effectively rendering the coupling coefficient P as a decreasing function of the delay T.

Equations (1), (2) have an equilibrium solution at

$$a = a_e = 1, \qquad b = b_e = 1 \quad (3)$$

Analyzing only bubble A, we may determine the stability of its equilibrium radius by setting $a = a_e + x = 1 + x$ and linearize about $x = 0$, giving

$$c\ddot{x} + 3\gamma\dot{x} + 3c\gamma x + P\dot{x}(t - T) = 0 \quad (4)$$

Note that, since c and γ are positive-valued parameters, if delay were absent from the model ($T = 0$), then Eq. (4) would correspond to a damped linear oscillator, which tells us that the equilibrium (3) would be stable. In the presence of delay, the characteristic equation must be solved to determine if any roots have positive real part.

Recently, the authors have studied Eqs. (1), (2), and developed explanations for their bifurcation structure, including the presence of Hopf [12] and Hopf–Hopf [24] bifurcations. However, these studies were limited in that they investigated only a small range of possible time delays. This work extends the previous by considering bifurcations that occur with larger delay.

2 Bifurcations of the in-phase mode

As studied previously [12, 26], the system (1), (2) possesses an invariant manifold called the in-phase manifold given by $a = b$, $\dot{a} = \dot{b}$. A periodic motion in the in-phase manifold is called an in-phase mode. The dynamics of the in-phase mode are governed by the equation [18]:

$$(\dot{a} - c)\left(a\ddot{a} + \frac{3}{2}\dot{a}^2 - a^{-3\gamma} + 1\right) - \dot{a}^3$$
$$- (3\gamma - 2)a^{-3\gamma}\dot{a} - 2\dot{a} = P\dot{a}(t - T) \quad (5)$$

We analyze the equilibrium of this equation $a = a_e = 1$ for Hopf bifurcations, giving rise to oscillations. When Hopf bifurcations occur, there will be a change in stability of the equilibrium point. To study the stability of the equilibrium point, we will analyze its linearization as provided in Eq. (4). This equation is a linear differential-delay equation. To solve it, we set $x = \exp \lambda t$ (see [15, 22]), giving

$$c\lambda^2 + 3\gamma\lambda + 3c\gamma = -P\lambda \exp -\lambda T \qquad (6)$$

We seek the values of delay $T = T_{cr}$, which cause instability. This will correspond to imaginary values of λ. Thus, we substitute $\lambda = i\omega$ in Eq. (6) giving two real equations for the real-valued parameters ω and T:

$$P\omega \sin \omega T = c(\omega^2 - 3\gamma) \qquad (7)$$

$$P\omega \cos \omega T = -3\gamma\omega \qquad (8)$$

Note that these equations have infinitely many solutions, as anticipated by the transcendental form of Eq. (6). In our previous work, only the first solution was studied. However, a further analysis of the bifurcation structure involves analyzing the full solution set to Eqs. (7), (8). We choose the following dimensionless parameters based on the papers by Keller et al. when numerics are required:

$$c = 94, \qquad \gamma = \frac{4}{3}, \qquad P = 10 \qquad (9)$$

The solutions to Eq. (6) are then found to be:

$$\omega_\alpha = \frac{\sqrt{P^2 - 9\gamma^2 + 12c^2\gamma} + \sqrt{P^2 + 9\gamma^2}}{2c} \approx 2.0493$$

$$\Rightarrow \quad T_\alpha = \frac{\arccos\left(\frac{-3\gamma}{10}\right) + 2\pi n}{\omega_\alpha} \quad (n \in \mathbb{Z}) \qquad (10)$$

$$\omega_\beta = \frac{\sqrt{P^2 - 9\gamma^2 + 12c^2\gamma} - \sqrt{P^2 + 9\gamma^2}}{2c} \approx 1.9518$$

$$\Rightarrow \quad T_\beta = \frac{-\arccos\left(\frac{-3\gamma}{10}\right) + 2\pi m}{\omega_\beta} \quad (m \in \mathbb{Z}) \quad (11)$$

Notice that, while there are only *two* frequencies ω_α, ω_β that solve the equations, each of them has an *infinite sequence* of T_α, T_β, respectively, that pairs with it as a solution. We will designate any delay T at which a Hopf bifurcation occurs as T_{cr}, independent of its corresponding frequency. Because of the solutions to Eqs. (7), (8) there will be two infinite sequences of
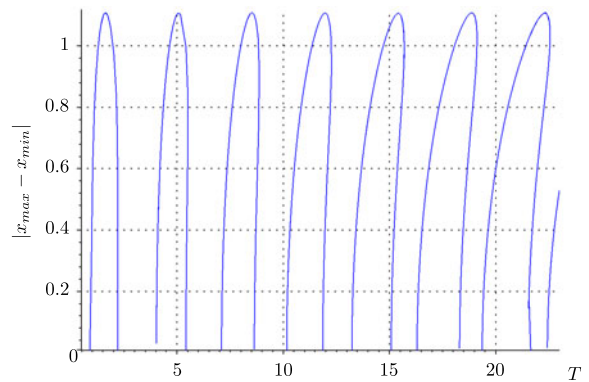

Fig. 2 Amplitude of limit cycle oscillations using numerical continuation of Eq. (5) for the parameter values in Eq. (9), with T as the continuation parameter. The Hopf bifurcations occur in a sequence where T_α is followed by T_β, and the two limit cycles coalesce in a saddle node of periodic orbits. The plot is continued in Fig. 3
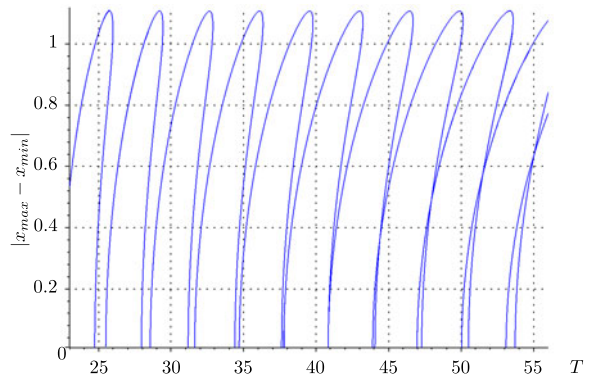

Fig. 3 Amplitude of limit cycle oscillations using numerical continuation of Eq. (5) for the parameter values in Eq. (9), with T as the continuation parameter. The Hopf bifurcations occur in a sequence where T_α is followed by T_β until $T \approx 44$, where two T_α-type Hopf bifurcations occur in a row. This is a continuation of Fig. 2

solutions that occur simultaneously. Each of the T_α, T_β delays correspond to Hopf bifurcations.

Using the numerical continuation package DDE-BIFTOOL [28], we present the amplitude of limit cycle oscillations that are born out of these sequences of Hopfs in Figs. 2 and 3. Note that the first Hopf bifurcation is of T_α-type, followed by one of T_β type. The two limit cycles born out of these Hopf bifurcations grow until they reach a radius at which the two coalesce and annihilate one another in a saddle-node of periodic orbits. The typical behavior in Fig. 2 is that a T_α-type Hopf always precedes a T_β-type Hopf.
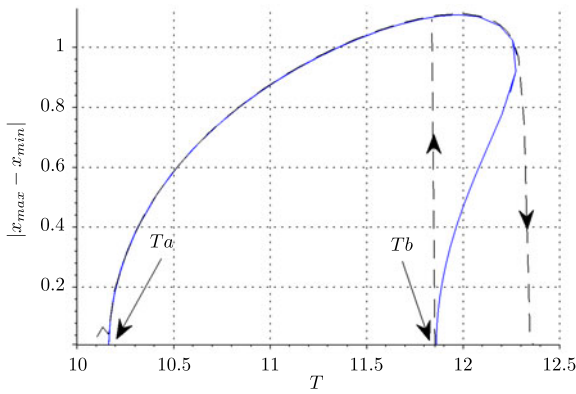
Fig. 4 A T_α-type Hopf bifurcation followed by a T_β-type. Here, the Hopf points are situated such that there is still a region where, after the two limit cycles are annihilated, the equilibrium point regains stability. *Solid lines* correspond to continuation whereas *dashed lines* correspond to jumps which show the stability of solutions as determined by numerical integration
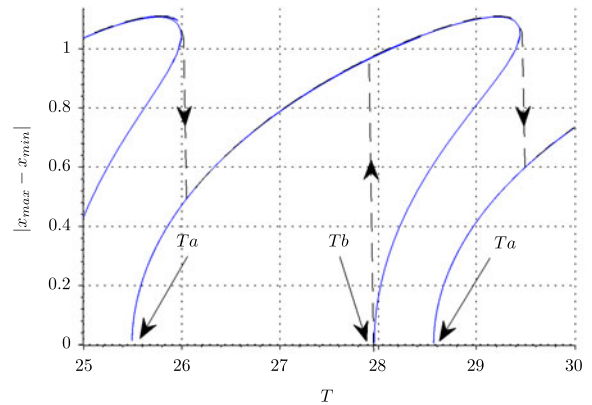
Fig. 5 A T_α-type Hopf bifurcation followed by a T_β-type, but with at least two limit cycles coexisting with the equilibrium point continuously throughout the parameter range. *Solid lines* correspond to continuation whereas *dashed lines* correspond to jumps which show the stability of solutions as determined by numerical integration
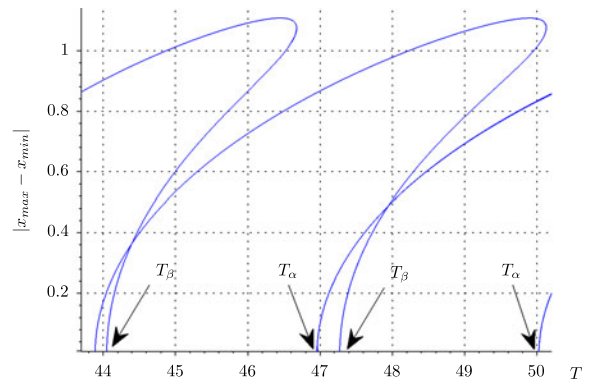

Fig. 6 For larger delay, the Hopf curves appear to meet as a result the reordering of the Hopf points at $T \approx 44$. *Solid lines* correspond to continuation; the jumps have been omitted

In Fig. 3, this ordering is reversed at $T \approx 44$. Here, another T_α-type Hopf bifurcation occurs prior to the T_β-type Hopf. This generic exchange in order of the two sequences has as a degenerate case the possibility that the two Hopf bifurcations align exactly, resulting in a Hopf–Hopf bifurcation. This phenomenon has been studied previously by means of center manifold reductions [24].

Next, we further examine Figs. 2 and 3 by characterizing representative regions of the figures. We recognize three distinct "regions" of qualitatively different behavior as the delay parameter increases. The first is presented in Fig. 4, which exhibits a sequence first of T_α resulting in limit cycle growth, followed by the incidence of T_β, which also spawns a limit cycle that meets the first Hopf curve in a saddle-node of periodic orbits. After the limit cycles are annihilated, the only invariant motion is the equilibrium point.

The region presented in Fig. 5 has the same bifurcation structure as that presented in Fig. 4, except that the trailing T_β-type Hopf bifurcation occurs close enough to the next T_α bifurcation such that for any delay value, there exists two stable periodic motions.

The region presented in Fig. 6 presents sophisticated behavior that is explored in greater depth by the authors through the use of an analogous system and the center manifold reduction method [24]. Just prior to this region (as apparent in Fig. 3), there is a reordering of the Hopf bifurcation sequence as a result of two T_α-type Hopfs occurring in a row at $T \approx 44$. This reordering is a possibility granted only by the infinite

number of roots for λ in Eq. (6) and the fact that Eq. (5) is an infinite-dimensional dynamical system. As a result, the behavior in Fig. 6 shows the Hopf curves apparently intersecting. It should be noted that each Hopf bifurcation occurs in its own two-dimensional center manifold, and these amplitude curves are only a projection of the dynamics of the system.

The primary focus of the forthcoming analysis is the case where the T_α- and T_β-type Hopfs follow each other in that order (i.e., regions corresponding to Figs. 4 and 5).

The Hopf bifurcations may be further characterized by their criticality. To analyze whether the bifurcations are supercritical or subcritical, regular perturbations

may be employed to characterize the motion of the associated eigenvalues. In particular, we begin with the characteristic equation (6) and let $T = T_{cr} + \mu_1$. Next, we establish perturbations on the eigenvalue:

$$\lambda = i\omega_{cr} + K_1\mu_1 + iK_2\mu_1 \tag{12}$$

That is, assume that $\Re(\lambda) = 0$ whenever $\mu_1 = 0$. Equating the real and imaginary parts of Eq. (6) with consideration of Eq. (12), and expanding for small μ_1 using computer algebra [16, 17] results in:

$$K_1\mu_1\left(-3c\omega_{cr}^2 + 3\gamma + 3c\right)$$
$$= -\omega_{cr}P\sin(T_{cr}\omega_{cr})$$
$$+ \left(\cos(T_{cr}\omega_{cr})\left(-\omega_{cr}^2 P - K_2 T_{cr}\omega_{cr}P - K_1 P\right)\right.$$
$$\left.+ \sin(T_{cr}\omega_{cr})(K_1 T_{cr}\omega_{cr}P - K_2 P)\right)\mu_1 \tag{13}$$

$$K_2\mu_1\left(-3c\omega_{cr}^2 + 3\gamma + 3c\right) + (3\gamma + 3c)\omega_{cr} + -c\omega_{cr}^3$$
$$= \mu_1\left(\cos(T_{cr}\omega_{cr})(K_1 T_{cr}\omega_{cr}P - K_2 P)\right.$$
$$\left.+ \sin(T_{cr}\omega_{cr})\left(\omega_{cr}^2 P + K_2 T_{cr}\omega_{cr}P + K_1 P\right)\right)$$
$$- \omega_{cr}P\cos(T_{cr}\omega_{cr}) \tag{14}$$

In solving for K_1, K_2 in terms of μ_1, we determine the "speed" at and direction in which the eigenvalues cross the imaginary axis. In particular, the sign of K_1 is of immediate interest; in particular, $K_1 > 0$ implies that the roots are moving from the left half-plane to the right half-plane, implying a stable origin becomes unstable. This is one of the conditions for a supercritical Hopf bifurcation.

Applying the conditions guaranteed by Eqs. (10), (11) subsequently into the expression for K_1 in Eq. (13) gives a long expression, for which we substitute in parameter values. For the first several ω_α-type Hopf bifurcations, the sequence of K_1 is provided in Table 1, whereas for the first several T_β-type Hopf bifurcations, the sequence of K_1 is provided in Table 2.

Given the exchange of stability that occurs at these Hopf bifurcations, we therefore conclude that the T_α values for delay correspond to supercritical Hopf bifurcations, whereas those corresponding to T_β correspond to subcritical bifurcations.

3 Stability of the in-phase mode

In the previous section, we established that in response to an increase in delay T, there is a bifurcation struc-

Table 1 Sequence of the first several T_α-type Hopf bifurcations and their corresponding values of K_1

n	T_{cr}	K_1
1	0.9673	0.0979
2	4.0332	0.0836
3	7.0992	0.0701
4	10.1651	0.0585
5	13.2311	0.0488
6	16.2970	0.0410
7	19.3630	0.0346

Table 2 Sequence of the first several T_β-type Hopf bifurcations and their corresponding values of K_1

n	T_{cr}	K_1
1	2.2035	−0.0840
2	5.4226	−0.0712
3	8.6417	−0.0595
4	11.8608	−0.0496
5	15.0799	−0.0415
6	18.2990	−0.0349
7	21.5181	−0.0296

ture, which alternates between supercritical and subcritical Hopf bifurcations. We drew this conclusion by analyzing the stability of the origin and inferring the stability of the periodic motion after bifurcation. However, there is a direct way to approach the stability of the in-phase mode by means of perturbations.

The two-variable expansion method is a well-known procedure for analyzing the amplitude and stability of limit cycles born in a Hopf bifurcation [15]. In a previous study, the authors performed second-order averaging [18] on the system for small delay. The two variable method is analogous to the second-order averaging approach and both methods will generate a set of differential equations for the amplitude and frequency of the limit cycle, as well as the approach of solutions that start sufficiently close to the limit cycle.

To begin, we introduce two variables: one fast, another slow:

$$\xi = \Omega t \tag{15}$$
$$\eta = \epsilon^2 t \tag{16}$$

Note that we expand immediately to $O(\epsilon^2)$; this is necessary because the nonlinearities are of quadratic order. This expansion will result in the following ap-

plications of the chain rule:

$$\frac{dx}{dt} = \Omega \frac{\partial x}{\partial \xi} + \epsilon^2 \frac{\partial x}{\partial \eta}$$

$$\frac{d^2 x}{dt^2} = \Omega^2 \frac{\partial^2 x}{\partial \xi^2} + 2\Omega \epsilon^2 \frac{\partial^2 x}{\partial \xi \partial \eta} + \epsilon^4 \frac{\partial^2 x}{\partial \eta^2} \tag{17}$$

Likewise, the time-delay term will also be affected by the chain rule [27]:

$$\dot{x}(t - T) = \Omega \frac{\partial x(\xi - \Omega T, \eta - \epsilon^2 T)}{\partial \xi}$$

$$+ \epsilon^2 \frac{\partial x(\xi - \Omega T, \eta - \epsilon^2 T)}{\partial \eta} \tag{18}$$

We now introduce another asymptotic series that builds a frequency-amplitude relationship into the limit cycle:

$$\Omega = \omega_{\mathrm{cr}} + \epsilon^2 k_2 \tag{19}$$

Now is the pivotal point at which we perturb off of the critical delay. This is done to eventually retrieve an asymptotic approximation for the dynamics of the system in the in-phase manifold past the Hopf bifurcation. In order to accomplish this, we set

$$T = T_{\mathrm{cr}} + \epsilon^2 \mu_2 \tag{20}$$

The quantity ΩT may be expanded, dropping terms smaller than $O(\epsilon^2)$:

$$\Omega T = \omega_{\mathrm{cr}} T_{\mathrm{cr}} + \epsilon^2 (\mu_2 \omega_{\mathrm{cr}} + k_2 T_{\mathrm{cr}}) + \cdots \tag{21}$$

In the derivation that follows, the shorthand $x_{\mathrm{d}} = x(\xi - \omega_{\mathrm{cr}} T_{\mathrm{cr}}, \eta)$ is adopted [25]. We wish to expand Eq. (18) taking into account Eq. (21). To fully expand this delay term in terms of its constituent derivatives, we note that:

$$\frac{\partial}{\partial \xi} x(\xi - \Omega T, \eta - \epsilon^2 T)$$

$$= \frac{\partial}{\partial \xi} x(\xi - (\omega_{\mathrm{cr}} + \epsilon^2 k_2)(T_{\mathrm{cr}} + \epsilon^2 \mu_2),$$

$$\eta - \epsilon^2 (T_{\mathrm{cr}} + \epsilon^2 \mu_2)) + \cdots$$

$$= \frac{\partial}{\partial \xi} x(\xi - \omega_{\mathrm{cr}} T_{\mathrm{cr}} - \epsilon^2 (k_2 T_{\mathrm{cr}} + \mu_2 \omega_{\mathrm{cr}}),$$

$$\eta - \epsilon^2 T_{\mathrm{cr}}) + \cdots$$

$$= \frac{\partial}{\partial \xi} x(\xi - \omega_{\mathrm{cr}} T_{\mathrm{cr}}, \eta)$$

$$- \epsilon^2 (k_2 T_{\mathrm{cr}} + \mu_2 \omega_{\mathrm{cr}}) \frac{\partial^2}{\partial \xi^2} x(\xi - \omega_{\mathrm{cr}} T_{\mathrm{cr}}, \eta)$$

$$- \epsilon^2 T_{\mathrm{cr}} \frac{\partial^2}{\partial \xi \partial \eta} x(\xi - \omega_{\mathrm{cr}} T_{\mathrm{cr}}, \eta) + \cdots$$

which we write as:

$$\frac{\partial}{\partial \xi} x(\xi - \Omega T, \eta - \epsilon^2 T)$$

$$= x_{\mathrm{d}_\xi} - \epsilon^2 x_{\mathrm{d}_{\xi\xi}} (k_2 T_{\mathrm{cr}} + \mu_2 \omega_{\mathrm{cr}}) - \epsilon^2 T_{\mathrm{cr}} x_{\mathrm{d}_{\xi\eta}} + \cdots$$

Therefore, the expansion for Eq. (18) is:

$$\dot{x}_d = (\omega_{\mathrm{cr}} + \epsilon^2 k_2) x_\xi (t - T) + \epsilon^2 x_\eta (t - T) + \cdots$$

$$= (\omega_{\mathrm{cr}} + \epsilon^2 k_2)(x_{\mathrm{d}_\xi} - \epsilon^2 x_{\mathrm{d}_{\xi\xi}} (k_2 T_{\mathrm{cr}} + \mu_2 \omega_{\mathrm{cr}})$$

$$- \epsilon^2 T_{\mathrm{cr}} x_{\mathrm{d}_{\xi\eta}} + \cdots) + \epsilon^2 x_{\mathrm{d}_\eta} + \cdots$$

$$= \omega_{\mathrm{cr}} x_{\mathrm{d}_\xi} - \epsilon^2 ((\mu_2 \omega_{\mathrm{cr}}^2 + k_2 T_{\mathrm{cr}} \omega_{\mathrm{cr}}) x_{\mathrm{d}_{\xi\xi}}$$

$$- k_2 x_{\mathrm{d}_\xi} + T_{\mathrm{cr}} \omega_{\mathrm{cr}} x_{\mathrm{d}_{\eta\xi}} - x_{\mathrm{d}_\eta}) + \cdots \tag{22}$$

Next, the solution to the differential equation is expanded in powers of ϵ:

$$x(\xi, \eta) = x_0(\xi, \eta) + \epsilon x_1(\xi, \eta) + \epsilon^2 x_2(\xi, \eta) + \cdots \tag{23}$$

Using Eqs. (23), (22) along with the perturbations (17), (19), and (20), the Taylor series expansion of Eq. (5) may be equated for the distinct orders of ϵ. This yields three equations ($O(1)$, $O(\epsilon)$, and $O(\epsilon^2)$):

$$L(x_0) = 0 \tag{24}$$

$$L(x_1) = \frac{1}{2c} ((2\omega_{\mathrm{cr}}^3 x_{0_\xi} - 2c\omega_{\mathrm{cr}}^2 x_0) x_{0_{\xi\xi}} - 3c\omega_{\mathrm{cr}}^2 x_{0_\xi}^2$$

$$+ 24\omega_{\mathrm{cr}} x_0 x_{0_\xi} + 20c x_0^2) \tag{25}$$

$$L(x_2) = -(4c^3 \omega_{\mathrm{cr}} x_{0_{\xi\eta}} + (2c^2 x_{0_\xi}^3 + 8x_{0_\xi}^3$$

$$+ 2P x_{0\mathrm{d}_\xi} x_{0_\xi}^2) \omega_{\mathrm{cr}}^3 + ((-3x_0 x_{0_\xi}^2 + 6x_{1_\xi} x_{0_\xi}) c^3$$

$$- 2P c^2 \mu_2 x_{0\mathrm{d}_{\xi\xi}} + (-24x_0 x_{0_\xi}^2$$

$$+ (16x_{1_\xi} - 2P x_{0\mathrm{d}_\xi} x_0 + 2P x_{1\mathrm{d}_\xi}) x_{0_\xi}$$

$$+ 2P x_{0\mathrm{d}_\xi} x_{1_\xi}) c) \omega_{\mathrm{cr}}^2$$

$$+ ((4c^3 x_{0_{\xi\xi}} - 2P T_{\mathrm{cr}} x_{0\mathrm{d}_{\xi\xi}} c^2) k_2$$

$$+ ((64x_0^2 - 24x_1) x_{0_\xi}$$

$$- 24x_0 x_{1_\xi} + 2P x_{0\mathrm{d}_\xi} x_0^2$$

$$- 2P x_{1\mathrm{d}_\xi} x_0 - 2P x_{0\mathrm{d}_\xi} x_1$$

$$-2Px_{0d_{\xi\eta}}T_{cr})c^2)\omega_{cr}$$
$$+(8x_{0_\xi}+2Px_{0d_\xi})c^2k_2$$
$$+(68x_0^3-56x_1x_0)c^3$$
$$+(8x_{0_\eta}+2Px_{0d_\eta})c^2)/(2c^3) \tag{26}$$

where

$$L(x_i)=\omega_{cr}^2 x_{i_{\xi\xi}}+\frac{4\omega_{cr}}{c}x_{i_\xi}+4x_i+\frac{P\omega_{cr}}{c}x_{id_\xi} \tag{27}$$

From (27) we see that $L(x_0)=0$ can be solved for x_{0d_ξ}, and using this, appearances of x_{0d} in Eq. (25) have been replaced by non-delayed values of x_0, x_{0_ξ}, and $x_{0_{\xi\xi}}$.

Equation (24) has the solution

$$x_0(\xi,\eta)=A(\eta)\cos(\xi)+B(\eta)\sin(\xi) \tag{28}$$

Inserting Eq. (28) into Eq. (25) and expanding appropriately gives the result:

$$L(x_1)=\left(\frac{\omega_{cr}^3-12\omega_{cr}}{2c}(A^2-B^2)\right.$$
$$\left.+\frac{5\omega_{cr}^2+20}{2}AB\right)\sin(2\xi)$$
$$+\left(\frac{5\omega_{cr}^2+20}{4}(A^2-B^2)\right.$$
$$\left.+\frac{12\omega_{cr}-\omega_{cr}^3}{c}AB\right)\cos(2\xi)$$
$$-\left(\frac{\omega_{cr}^2-20}{4}\right)(A^2+B^2) \tag{29}$$

Note that $L(x_1)$ has no secular terms since all $O(\epsilon)$ terms are quadratic, as expected. Eq. (25) has the solution:

$$x_1(\xi,\eta)=C(\eta)\cos(\xi)+D(\eta)\sin(\xi)$$
$$+E(\eta)\cos(2\xi)+F(\eta)\sin(2\xi)+G(\eta) \tag{30}$$

where the coefficients C, D are arbitrary functions of η, and where E, F, and G are known functions of A and B. We substitute Eq. (30) for x_1 into Eq. (26) and eliminate resonance terms by equating to zero the coefficients of $\cos(\xi)$ and $\sin(\xi)$. Doing so yields the "slow flow" equations on coefficients A and B. The slow flow equations on A and B both contain 588

terms, so we omit printing them here. However, the equations are all of the form

$$\frac{dA}{d\eta}=Y_{111}A^3+Y_{112}A^2B+Y_{121}AB^2+Y_{122}B^3$$
$$+Y_{101}A+Y_{102}B \tag{31}$$
$$\frac{dB}{d\eta}=Y_{211}A^3+Y_{212}A^2B+Y_{221}AB^2+Y_{222}B^3$$
$$+Y_{201}A+Y_{202}B \tag{32}$$

where Y_{ijk} are all constant functions depending on the parameters c, P and T_{cr}, ω_{cr}.

In order to solve the system of Eqs. (31), (32), we transform the problem to polar coordinates, setting:

$$A(\eta)=R(\eta)\cos(\theta(\eta))$$
$$B(\eta)=R(\eta)\sin(\theta(\eta))$$

This results in a slow flow equation of the form

$$\frac{dR}{d\eta}=\Gamma_1 R^3-\Gamma_2\mu_2 R \tag{33}$$
$$\frac{d\theta}{d\eta}=\Gamma_3 R^2+\Gamma_4\mu_2+k_2 \tag{34}$$

where the Γ_i are known constants.

Equilibria of the slow flow equations correspond to limit cycles in the full system. The nontrivial equilibrium point for Eq. (33) will give a prediction for the amplitude of the corresponding limit cycle depending on μ_2. We choose k_2 such that when Eq. (33) is at equilibrium for some R_{eq}, then $\frac{d\theta}{d\eta}=0$ in Eq. (34). Table 3 provides results of the perturbation method for the given T_α parameter values.

Finally, we note that for the Hopf bifurcations in Table 3, Γ_1 and Γ_2 are both positive. This shows that

Table 3 Results of the Two-Variable Expansion method for the parameter values $P=10, \gamma=\frac{4}{3}$ on Eq. (5) where $\Delta=\epsilon^2\mu_2=T-T_{cr}$

n	T_{cr}	$R_{eq}/\sqrt{\Delta}$	k_2/Δ
0	0.9672	1.4523	−1.4506
1	4.0332	0.81566	−0.45758
2	7.0991	0.62844	−0.27136
3	10.165	0.52993	−0.19314
4	13.231	0.46676	−0.14984
5	16.297	0.42187	−0.12240
6	19.362	0.38784	−0.10346
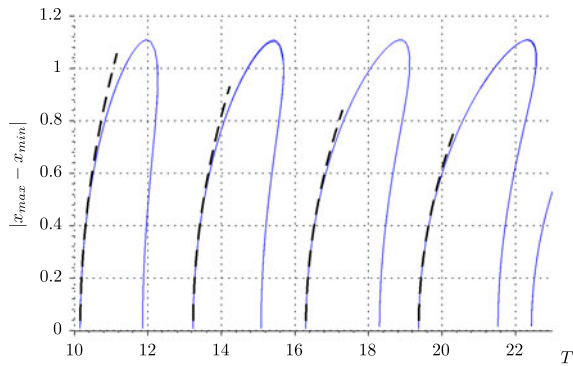
Fig. 7 Continuation and perturbation methods compared for a series of Hopf points. *Dashed lines* correspond to perturbation results, whereas *solid lines* correspond to continuation

limit cycles occur for $\mu_2 > 0$. Furthermore, it confirms our earlier analysis suggesting that Hopf bifurcations which occur with time delay T_α are supercritical because linearization about the equilibrium radius R_{eq} yields that the equilibrium point of the slow flow (corresponding to the limit cycle that is the in-phase mode) is stable.

A comparison of these results with numerical continuation is provided in Fig. 7. The continuation curves were generated using `DDE-BIFTOOL`.

4 Stability of the in-phase manifold

While the above analysis has ascertained that, for the Hopf bifurcations associated with time delay T_α, the in-phase mode is stable, the question remains for the original equations (1), (2) whether the motion is stable. That is, we have so far analyzed the dynamics only when restricted to the initial conditions $a = b$, $\dot{a} = \dot{b}$, and we have ascertained the local stability of the in-phase mode restricted to this space. However, if more general initial conditions are considered, will the periodic motions born out of the supercritical Hopf bifurcations be stable?

To answer this question, we will no longer restrict our analysis to the in-phase manifold equation (5) and instead will investigate the full system (1), (2). We will again recognize that these equations exhibit the equilibrium solution $a_e = b_e = 1$, so we will look at deviations from that motion. We set $a = a_e + \epsilon x$, $b = b_e + \epsilon y$, solve for $\ddot{x}$ and take the Taylor series approximation for the system for small ϵ. After dividing both

sides by a shared factor of ϵ, this will transform the system (1), (2) into:

$$
\begin{aligned}
c\ddot{x} &+ 4\dot{x} + 4cx + P\dot{y}(t - T) \\
&= \frac{1}{2c}\big(\big((28x^2 - 3\dot{x}^2)c^2 \\
&\quad + c\big(24\dot{x} + 2P\dot{y}(t - T)\big)x \\
&\quad - 8\dot{x}^2 - 2P\dot{y}(t - T)\dot{x}\big)\epsilon\big) \\
&\quad - \frac{1}{2c^2}\big(c^3\big(68x^3 - 3\dot{x}^2 x\big) \\
&\quad + c^2\big(\big(64\dot{x}x^2 + 2P\dot{y}(t - T)\big)x^2 + 2\dot{x}^3\big) \\
&\quad + c\big(-24\dot{x}^2 - 2P\dot{y}(t - T)\dot{x}\big)x + 8\dot{x}^3 \\
&\quad + 2P\dot{y}(t - T)\dot{x}^2\big)\epsilon^2 + \mathcal{O}\big(\epsilon^3\big)
\end{aligned}
\tag{35}
$$

$$
\begin{aligned}
c\ddot{y} &+ 4\dot{y} + 4cy + P\dot{x}(t - T) \\
&= \frac{1}{2c}\big(\big((28y^2 - 3\dot{y}^2)c^2 \\
&\quad + c\big(24\dot{y} + 2P\dot{x}(t - T)\big)y \\
&\quad - 8\dot{y}^2 - 2P\dot{x}(t - T)\dot{y}\big)\epsilon\big) \\
&\quad - \frac{1}{2c^2}\big(c^3\big(68y^3 - 3\dot{y}^2 y\big) \\
&\quad + c^2\big(\big(64\dot{y}y^2 + 2P\dot{x}(t - T)\big)y^2 + 2\dot{y}^3\big) \\
&\quad + c\big(-24\dot{y}^2 - 2P\dot{x}(t - T)\dot{y}\big)y + 8\dot{y}^3 \\
&\quad + 2P\dot{x}(t - T)\dot{y}^2\big)\epsilon^2 + \mathcal{O}\big(\epsilon^3\big)
\end{aligned}
\tag{36}
$$

Note that we have already substituted $\gamma = \frac{4}{3}$ from Eq. (9). In the nomenclature of the above formulation, Eqs. (1), (2) support a Hopf bifurcation in the in-phase manifold $x = y = f(t)$ (the periodic motion):

$$
\begin{aligned}
c\ddot{f} &+ 4\dot{f} + 4cf + P\dot{f}(t - T) \\
&= \frac{1}{2c}\big(\big((28f^2 - 3\dot{f}^2)c^2 \\
&\quad + c\big(24\dot{f} + 2P\dot{f}(t - T)\big)f \\
&\quad - 8\dot{f}^2 - 2P\dot{f}(t - T)\dot{f}\big)\epsilon\big) \\
&\quad - \frac{1}{2c^2}\big(c^3\big(68f^3 - 3\dot{f}^2 f\big) \\
&\quad + c^2\big(\big(64\dot{f}f^2 + 2P\dot{f}(t - T)\big)f^2 + 2\dot{f}^3\big) \\
&\quad + c\big(-24\dot{f}^2 - 2P\dot{f}(t - T)\dot{f}\big)f + 8\dot{f}^3 \\
&\quad + 2P\dot{f}(t - T)\dot{f}^2\big)\epsilon^2 + \mathcal{O}\big(\epsilon^3\big)
\end{aligned}
\tag{37}
$$

We have found the approximate solution of Eq. (37) for $c = 94$, $P = 10$, and $T = T_{cr} + \Delta$ to be

$$f(t) = R_{eq} \cos\left((\omega_{cr} + \epsilon^2 k_2)t\right) \tag{38}$$

where R_{eq}, k_2 are calculated in the previous section for delays T_{cr} corresponding to supercritical Hopfs; see Table 3. The goal is to determine the stability of the motion $f(t)$ in Eq. (38). To do this, one may analyze the linear variational equations of Eqs. (35), (36). Setting $x = \delta x + f$, $y = \delta y + f$ and expanding for small $\delta x, \delta y$ results in the linear variational equations shown in Eqs. (39), (40). Note that here the notation $\dot{x}_d = \dot{x}(t - T_{cr})$ and the same for y is used.

$$c\delta\ddot{x} + 4c\delta\dot{x} + 4\delta x + P\delta\dot{y}_d$$
$$= -\frac{1}{c}\big((3\dot{f}\delta\dot{x} - 28f\delta x)c^2$$
$$+ \big(-12f\delta\dot{x} + (-P\dot{f}_d - 12\dot{f})\delta x - fP\delta\dot{y}_d\big)c$$
$$+ (P\dot{f}_d + 8\dot{f})\delta\dot{x} + P\dot{f}\delta\dot{y}_d)\epsilon$$
$$+ \big(\big(\big(6f\dot{f}\delta\dot{x} + (3\dot{f}^2 - 204f^2)\delta x\big)c^3$$
$$+ \big(\big(-6\dot{f}^2 - 64f^2\big)\delta\dot{x}$$
$$- (4Pf\dot{f}_d + 128f\dot{f})\delta x - 2Pf^2\delta\dot{y}_d\big)c^2$$
$$+ \big((2Pf\dot{f}_d + 48f\dot{f})\delta\dot{x}$$
$$+ \big(2P\dot{f}_d\dot{f} + 24\dot{f}^2\big)\delta x + 2Pf\dot{f}\delta\dot{y}_d\big)c$$
$$- (4P\dot{f}_d\dot{f} + 24\dot{f}^2)\delta\dot{x}$$
$$- 2P\dot{f}^2\delta\dot{y}_d\big)\epsilon^2\big)/(2c^2) + \mathcal{O}(\epsilon^3) \tag{39}$$

$$c\delta\ddot{y} + 4c\delta\dot{y} + 4\delta y + P\delta\dot{x}_d$$
$$= -\frac{1}{c}\big((3\dot{f}\delta\dot{y} - 28f\delta y)c^2$$
$$+ \big(-12f\delta\dot{y} + (-P\dot{f}_d - 12\dot{f})\delta y - fP\delta\dot{x}_d\big)c$$
$$+ (P\dot{f}_d + 8\dot{f})\delta\dot{y} + P\dot{f}\delta\dot{x}_d)\epsilon$$
$$+ \big(\big(\big(6f\dot{f}\delta\dot{y} + (3\dot{f}^2 - 204f^2)\delta y\big)c^3$$
$$+ \big(\big(-6\dot{f}^2 - 64f^2\big)\delta\dot{y}$$
$$- (4Pf\dot{f}_d + 128f\dot{f})\delta y - 2Pf^2\delta\dot{x}_d\big)c^2$$
$$+ \big((2Pf\dot{f}_d + 48f\dot{f})\delta\dot{y}$$
$$+ \big(2P\dot{f}_d\dot{f} + 24\dot{f}^2\big)\delta y + 2Pf\dot{f}\delta\dot{x}_d\big)c$$
$$- (4P\dot{f}_d\dot{f} + 24\dot{f}^2)\delta\dot{y}$$
$$- 2P\dot{f}^2\delta\dot{x}_d\big)\epsilon^2\big)/(2c^2) + \mathcal{O}(\epsilon^3) \tag{40}$$

To analyze Eqs. (39), (40), we set $u = \delta x - \delta y$ and $v = \delta x + \delta y$ in order to transform the problem into "in-phase" and "out-of-phase" coordinates. We then add and subtract Eqs. (39), (40) to and from one another respectively to obtain

$$c\ddot{u} + 4\dot{u} + 4uc - P\dot{u}_d$$
$$= \frac{1}{c}\big((\dot{f} - cf)P\dot{u}_d$$
$$+ \big(-\dot{f}_dP + (-3c^2 - 8)\dot{f} + 12cf\big)\dot{u}$$
$$+ \big(c\dot{f}_dP + 12c\dot{f} + 28c^2f\big)u\big)\epsilon$$
$$+ \big(\big(\big(2\dot{f}^2 - 2cf\dot{f} + 2c^2f^2\big)P\dot{u}_d$$
$$+ \big((-4\dot{f} + 2cf)\dot{f}_dP$$
$$+ \big(-6c^2 - 24\big)\dot{f}^2 + \big(6c^3 + 48c\big)f\dot{f} - 64c^2f^2\big)\dot{u}$$
$$+ \big((2c\dot{f} - 4c^2f)\dot{f}_dP + (3c^3 + 24c)\dot{f}^2$$
$$- 128c^2f\dot{f} - 204c^3f^2\big)u\big)\epsilon^2\big)/(2c^2) + \mathcal{O}(\epsilon^3) \tag{41}$$

$$c\ddot{v} + 4\dot{v} + 4vc + P\dot{v}_d$$
$$= -\frac{1}{c}\big((\dot{f} - cf)P\dot{v}_d$$
$$+ \big(\dot{f}_dP + (3c^2 + 8)\dot{f} - 12cf\big)\dot{v}$$
$$+ \big(-c\dot{f}_dP - 12c\dot{f} - 28c^2f\big)v\big)\epsilon$$
$$- \big(\big(\big(2\dot{f}^2 - 2cf\dot{f} + 2c^2f^2\big)P\dot{v}_d$$
$$+ \big((4\dot{f} - 2cf)\dot{f}_dP + (6c^2 + 24)\dot{f}^2$$
$$+ \big(-6c^3 - 48c\big)f\dot{f} + 64c^2f^2\big)\dot{v}$$
$$+ \big((-2c\dot{f} + 4c^2f)\dot{f}_dP + (-3c^3 - 24c)\dot{f}^2$$
$$+ 128c^2f\dot{f} + 204c^3f^2\big)v\big)\epsilon^2\big)/(2c^2) + \mathcal{O}(\epsilon^3) \tag{42}$$

Inspection shows that Eq. (42) is the variational equation of Eq. (37). Because of this, it is seen that v determines the stability of the motion $x = y = f(t)$ *in* the in-phase manifold, while u determines the stability *of* the in-phase manifold. Since Eq. (42) is a linear delay-differential equation, its solution space is spanned by an infinite number of linearly independent solutions. One of these solutions is $v = \frac{df}{dt}$, as may be seen by differentiating Eq. (37) and comparing with Eq. (42). The solution is periodic since $f(t)$ is periodic. All other solutions of Eq. (42) are expected to be

asymptotically stable for small ϵ, since as proven in the previous section, $f(t)$ is a limit cycle born in a supercritical Hopf bifurcation. Therefore, the stability of the in-phase mode $x = y = f(t)$ is determined solely by Eq. (41).

It is notable that a basic difference between Eqs. (41) and (42) is that when $\epsilon = 0$, Eq. (42) exhibits a periodic solution (due to the Hopf bifurcation), while Eq. (41) does not. Thus, at $\epsilon = 0$, Eq. (42) is structurally unstable, whereas Eq. (41) is structurally stable. Therefore, for small values of ϵ, the stability of Eq. (41) is the same as it is for $\epsilon = 0$. The stability of Eq. (41) (and of the in-phase mode $x = y = f(t)$) is then determined by the behavior of the $\epsilon = 0$ version of Eq. (41):

$$c\ddot{u} + 4\dot{u} + 4cu - P\dot{u}(t - T_{\text{cr}}) = 0 \qquad (43)$$

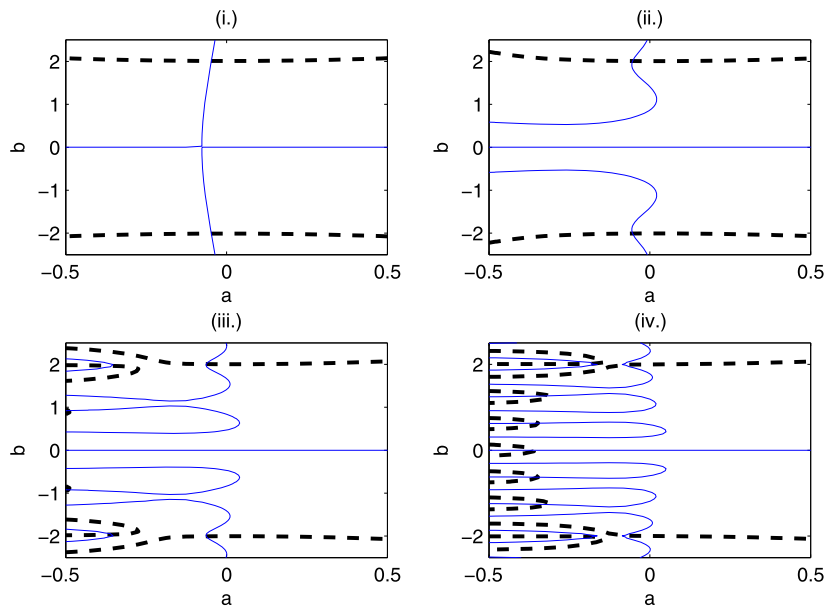To solve Eq. (43), set $u = \exp(\lambda t)$ and obtain the characteristic equation

$$c\lambda^2 + 4\lambda + 4c\lambda - P\exp(-\lambda T_{\text{cr}}) = 0 \qquad (44)$$

Writing $\lambda = a + ib$ and equating imaginary and real parts yields:

$$0 = P\exp(-aT_{\text{cr}})\sin(bT_{\text{cr}}) + 4b + 2abc \qquad (45)$$

$$0 = P\exp(-aT_{\text{cr}})\cos(bT_{\text{cr}}) - 4a + c(b^2 - a^2 - 4) \qquad (46)$$

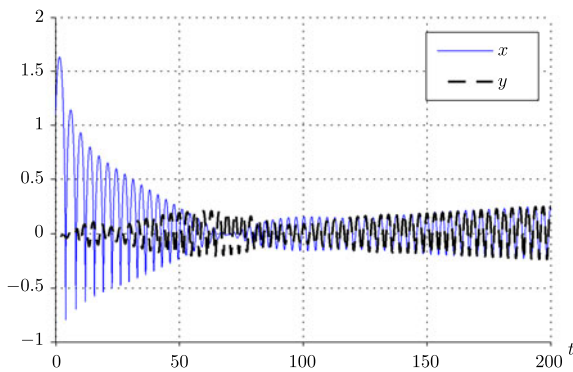For stability, all roots to Eqs. (45), (46) must have $a < 0$. For instability, there must be at least one root for which $a > 0$.

Figure 8 shows plots of the implicit functions in Eqs. (45), (46), where intersections of the curves designate solutions to the system of simultaneous equations. Inspection shows that there are no roots for which $a > 0$, showing that the in-phase mode is stable. These plots are only shown for the first few values of delay for which their is a supercritical Hopf bifurcation.

This conclusion is supported by numerical integration using the MATLAB toolbox dde23, for which we show a characteristic time integration in Fig. 9. The time integration features an arbitrary choice of initial conditions off the in-phase manifold, and it is witnessed that the solution approaches the in-phase mode.

5 Conclusion

This work has investigated the stability of periodic motions that arise from a differential-delay equation associated with the coupled dynamics of two oscillating bubbles. The delayed dynamics arise as a result of the finite speed of sound in the surrounding fluid, leading to a nonnegligible propagation time for waves created by one bubble to reach the other.

Fig. 8 Plot of the curves in Eqs. (45), (46) for
(i.) $T_{\text{cr}} = 0.96734$,
(ii.) $T_{\text{cr}} = 4.03324$,
(iii.) $T_{\text{cr}} = 7.09919$, and
(iv.) $T_{\text{cr}} = 10.165$.
Solid lines are plots of Eq. (45), *dashed lines* are plots of Eq. (46)

Fig. 9 Time series integration for arbitrary initial conditions (here, $(x_0, \dot{x}_0, y_0, \dot{y}_0) = (1.1, 0, 0.8, 0)$) for the bubble equation just past a supercritical Hopf bifurcation with $T = 4.2$

The main focus of study for the problem is the invariant manifold on which the bubble dynamics are identical, which is termed the "in-phase manifold." The study investigated the dynamics of the in-phase manifold, particularly around the equilibrium radius of the bubble. It is shown that this equilibrium point undergoes a Hopf bifurcation in response to a change in delay T giving rise to limit cycles. There are two sequences of Hopf bifurcations that occur at distinct intervals, with one shown to be always supercritical while the other subcritical. The supercritical Hopf bifurcations are further characterized by use of the two-variable expansion method, which provides a formal prediction for amplitude and frequency of oscillations based on the delay parameter.

With the stability picture of the in-phase mode on the in-phase manifold established, the stability of the manifold itself is then established. Through the use of linear variational equations for the periodic motion born in the Hopf bifurcation, it is shown that for arbitrary initial conditions near the in-phase mode, all motions will approach the in-phase manifold. Therefore, the analysis of the in-phase mode is complete; it is determined that, when it exists, the in-phase mode is stable.

References

1. Dijkmans, P.A., et al.: Microbubbles and ultrasound: from diagnosis to therapy. Eur. J. Echocardiogr. **5**, 245–256 (2004)

2. Doinikov, A.A., Manasseh, R., Ooi, A.: Time delays in coupled multibubble systems. J. Acoust. Soc. Am. **117**, 47–50 (2005)

3. Ferrara, K., Pollard, R., Borden, M.: Ultrasound microbubble contrast agents: fundamentals and application to gene and drug delivery. Annu. Rev. Biomed. Eng. **9**, 415–447 (2007)

4. Gilmore, F.R.: "The growth or collapse of a spherical bubble in a viscous compressible liquid". Report no. 26-4, Hydrodynamics Laboratory, California Institute of Technology, Pasadena, California (1952)

5. Harkin, A., Kaper, T., Nadim, A.: Coupled pulsation and translation of two gas bubbles in a liquid. J. Fluid Mech. **445**, 377–411 (2001)

6. Keller, J.B., Kolodner, I.I.: Damping of underwater explosion bubble oscillations. J. Appl. Phys. **27**, 1152–1161 (1956)

7. Keller, J.B., Miksis, M.: Bubble oscillations of large amplitude. J. Acoust. Soc. Am. **68**, 628–633 (1980)

8. Lauterborn, W., Parlitz, U.: Methods of chaos physics and their application to acousticse. J. Acoust. Soc. Am. **84**(6), 1975–1993 (1988)

9. Leighton, T.G.: From sea to surgeries, from babbling brooks to baby scans: bubble acoustics at ISVR. Proc. Inst. Acoust. **26**, 357–381 (2004)

10. Manasseh, R., Nikolovska, A., Ooi, A., Yoshida, S.: Anisotropy in the sound field generated by a bubble chain. J. Sound Vib. **278**, 807–882 (2004)

11. Mettin, R.: Dynamics of delay-coupled spherical bubbles. In: Lauterborn, W., Kurz, T. (eds.) Proceedings of the 15th International Symposium on Nonlinear Acoustics Göttingen, Germany 1–4 Sept. (1999)

12. Heckman, C.R., Sah, S.M., Rand, R.H.: Dynamics of microbubble oscillators with delay coupling. Commun. Nonlinear Sci. Numer. Simul. **15**, 2735–2743 (2010)

13. Plesset, M.S.: The dynamics of cavitation bubbles. J. Appl. Mech. **16**, 277–282 (1949)

14. Plesset, M.S., Prosperettti, A.: Bubble dynamics and cavitation. Annu. Rev. Fluid Mech. **9**, 145–185 (1977)

15. Rand, R.H.: Lecture Notes in Nonlinear Vibrations, version 53. Published on-line by the Internet-First University Press (2012) http://ecommons.library.cornell.edu/handle/1813/28989

16. Rand, R.H., Armbruster, D.: Perturbation Methods, Bifurcation Theory, and Computer Algebra. Springer, New York (1987)

17. Rand, R.H.: Topics in Nonlinear Dynamics with Computer Algebra. Gordon and Breach Science, Langhorne (1994)

18. Rand, R.H., Heckman, C.R.: Dynamics of coupled bubble oscillators with delay. In: Proceedings of ASME 2009 IDETC/CIE 2009, August 30–September 2, 2009, San Diego, California

19. Rayleigh, L.: On the pressure developed in a liquid during the collapse of a spherical cavity. Philos. Mag. **34**, 94–98 (1917)

20. Reddy, A.J., Szeri, A.J.: Coupled dynamics of translation and collapse of acoustically driven microbubbles. J. Acoust. Soc. Am. **112**, 1346–1352 (2002)

21. Toilliez, J.O., Szeri, A.J.: Optimized translation of microbubbles driven by acoustic fields. J. Acoust. Soc. Am. **123**, 1916–1930 (2008)

22. Wirkus, S., Rand, R.: Dynamics of two coupled Van Der Pol oscillators with delay coupling. Nonlinear Dyn. **30**, 205–221 (2002)
23. Yamakoshi, Y., Ozawa, Y., Ida, M., Masuda, N.: Effects of Bjerknes forces on Gas-Filled microbubble trapping by ultrasonic waves. Jpn. J. Appl. Phys. **40**, 3852–3855 (2001)
24. Heckman, C.R., Rand, R.H.: Asymptotic analysis of the Hopf-Hopf bifurcation in a time-delay system. J. Appl. Nonlinear Dyn. **1**(2), 159–171 (2012)
25. Suchorsky, M.K., Sah, S.M., Rand, R.H.: Using delay to quench undesirable vibrations. Nonlinear Dyn. **62**, 107–116 (2010)
26. Heckman, C.R., Rand, R.H.: Dynamics of coupled microbubbles with large fluid compressibility delays. In: Proc. EUROMECH 2011 Euro. Nonlin. Osc. Conf
27. Rand, R.H.: Differential-Delay equations. In: Luo, A.C.J., Sun, J.-Q. (eds.) Complex Systems: Fractionality, Time-delay and Synchronization, pp. 83–117. Springer, Berlin (2011)
28. Engelborghs, K., Luzyanina, T., Samaey, G., Roose, D., Verheyden, K.: DDE-BIFTOOL. Available from http://twr.cs.kuleuven.be/research/software/delay/ddebiftool.shtml